PCCP

Accepted Manuscript

ROYAL SOCIETY OF CHEMISTRY

www.rsc.org/pccp

PCCP

RSCPublishing

ARTICLE

Cite this: DOI: 10.1039/x0xx00000x

Solvation Dynamics and Energetics of Intramolecular Hydride Transfer Reactions in Biomass Conversion

Samir H. Mushrif,[a]* Jithin J. Varghese,[a†] Chethana B. Krishnamurthy[a†]

Received ooth January 2012,
Accepted ooth January 2012

DOI: 10.1039/x0xx00000x

www.rsc.org/

Hydride transfer changes the charge structure of the reactant and thus, may induce reorientation/reorganization of solvent molecules. This solvent reorganization may in turn alter the energetics of the reaction. In the present work, we investigate the intramolecular hydride transfer by taking Lewis acid catalyzed glucose to fructose isomerization as an example. The C_2–C_1 hydride transfer is the rate limiting step in this reaction. Water and methanol are used as solvents and hydride transfer is simulated in the presence of explicit solvent molecules, treated quantum mechanically and at a finite temperature, using Car–Parrinello molecular dynamics (CPMD) and metadynamics. Activation free energy barrier for hydride transfer in methanol is found to be 50 kJ/mol higher than that in water. On the contrary, in density functional theory calculations, using implicit solvent environment, the barriers are almost identical. Analysis of solvent dynamics and electronic polarization along the molecular dynamics trajectory and the results of CPMD–metadynamics simulation of the hydride transfer process in the absence of any solvent suggest that higher barrier in methanol is a result of non–equilibrium solvation. Methanol undergoes electronic polarization during the hydride transfer step; however, its molecular orientational relaxation is a much slower process that takes place after the hydride transfer, over an extended timescale, resulting in non–equilibrium solvation. Water, on the other hand, does not undergo significant electronic polarization and thus, has to undergo minimal reorientation to provide near equilibrium solvation to the transition state and an improved equilibrium solvation to the post hydride shift product state. Hence, the hydride transfer step is also observed to be exergonic in water and endergonic in methanol. The aforementioned explanation is juxtaposed to enzyme catalyzed charge transfer reactions, where the enhanced solvation of the transition and product states by enzymes, due to electrostatic interactions, reduces the activation free energy barrier and the free energy change of the reaction. Similarly, we suggest that, in the intramolecular hydride shift, improved solvation of the transition state and of the product state by water is achieved due to minimal polarization and reorientation, and (near) equilibrium solvation.

Introduction

Intramolecular hydride transfer is a commonly observed, and usually the rate limiting step in some of the key Lewis and Brønsted acid catalyzed biomass reactions, like isomerization and dehydration, respectively.[1-9] Since cellulosic biomass and its sugar derivatives are solid species, these reactions are performed in a solvent medium. Though water is the most preferred solvent, experimental studies have shown that the addition of a co–solvent to water or replacing water with an alternate solvent can significantly alter conversions and selectivities in these reactions.[10-15] It is believed that solvents can play dual role in biomass reactions. (i) A solvent can either preferentially solvate an "active" functional group of a biomass molecule or its derivative and protect it from taking part into the reaction, thus precluding a particular reaction pathway. For example, in the dehydration reaction of fructose to 5–hydroxymethyl furfural (HMF), it has been shown that an aprotic solvent like dimethyl sulfoxide (DMSO) preferentially solvates the carbonyl (–C=O) group of HMF. This specific arrangement of DMSO around HMF is likely to protect HMF from getting rehydrated to levulinic and formic acids and from forming condensation products like humins, thus leading to an increased yield of HMF.[16-19] (ii) On the other hand, solvent can also directly participate in the reaction. For example, theoretical investigations have shown that water could be responsible to mediate proton transfers in biomass reactions;[20] in basic pH conditions, hydroxide ions in water can provide oxygen for catalytic oxidation reactions;[21] a hydrogen bonded water molecule can act as a catalyst in the isomerization reaction.[22] Kinetic experiments have also suggested that activation energy barriers for glucose dehydration and condensation reactions change systematically with changing solvent composition.[23, 24] Additionally, sugars can introduce acidity in the solvent and it

is believed that this effect is also dependant on the solvent environment.[25]

Solvent dynamics can also play a major role in altering the kinetics of sugars isomerization and dehydration reactions, since they involve charge transfer steps like hydride transfer.[4, 20, 26] Charge transfer within the reactant (sugar) changes the electronic and orientational dipole of the reactant and thus, the solvent needs to reorganize itself accordingly. Though there are multiple theoretical investigations which have observed the effect of solvent environment on activation barriers for hydride transfer and charge transfer reactions, in general, in biomass molecules,[6, 23, 27] very few made an attempt to address the importance of solvent dynamics.[4, 5, 9, 20] Caratzoulas et al.[4], investigated the dehydration of fructose to HMF in a condensed phase environment in which they treated solvent water molecules explicitly using molecular mechanics. They observed that intramolecular hydride transfer is the rate limiting step in the mechanism and that the electrostatic component of the internal energy of the solvent contributes most to the activation free energy barrier associated with it. Based on this observation, they suggested that solvent reorientation could be responsible for the high barrier for hydride transfer. Later, the same group also developed a microkinetic model[5] for the reaction and demonstrated that experimental reaction kinetics can only be predicted accurately if Marcus theory rate constants are used for the rate limiting hydride transfer step.

Another factor that could play a role in altering the energetics of hydride transfer is the non–equilibrium solvation. Non–equilibrium solvation occurs when the electronic degrees of freedom of the solvent are able to align themselves almost instantly with the change in the charge distribution of the solute, but the orientational degrees of freedom (for ex. rotational) remain equilibrated with the original charge distribution, since their relaxation timescales are significantly longer. To the best of our knowledge, there are no reports investigating the effect of solvent dynamics and non–equilibrium solvation on intramolecular hydride transfer (or charge transfer, in general) step in biomass reactions, where solvent molecules are either treated quantum mechanically or are modeled using an appropriate polarizable force–field that can capture the polarization response of the solvent. Hence, it has not yet been possible to estimate or to comment on the contribution of the solvent reorganization energy to the activation energy barrier for such reactions.

The present paper attempts to investigate solvation dynamics and non–equilibrium solvation effect on the intramolecular hydride transfer reaction in sugar molecules, taking the C_2 to C_1 hydride transfer in a Lewis acid catalyzed glucose to fructose isomerization reaction as an example. *Ab initio* molecular dynamics calculations are performed, where the entire reaction system, including the solvent molecules, is treated quantum mechanically. Details of the simulation system and computational methods are given in the next section. The hydride transfer step is studied in two solvents with different polarizabilities and polarities, i.e., water and methanol. The results elucidating the effect of the solvent environment on the energetics of the hydride transfer step and the analysis of the simulation data suggesting a possible role of solvent dynamics and non–equilibrium solvation are discussed in the results and discussion section. We conclude our findings at the end.

Simulation System and Computational Methods

Simulation system

Since the present paper only focuses on the hydride transfer step, the entire isomerization reaction mechanism, which is well accepted in the literature,[1, 3, 8] was not simulated. The partially hydrolyzed Sn–defect site, where Sn is tetrahedrally attached to 3 oxygens of the zeolite framework and with an –OH group,[2, 28-33] was taken as the catalyst. The first step in the isomerization reaction is the coordination of glucose to the Sn–metal center and the formation of an octahedral complex, where Sn is also coordinated with C_1 carbonyl and C_2 hydroxyl groups of glucose (*cf* Fig. 1a). Before the hydride transfer, glucose gets deprotonated at the C_2–OH group and the Sn–OH defect site accepts that proton, leading to the formation of an incipient water molecule that remains coordinated to Sn. Sn forms a covalent bond with C_2 oxygen; C_2–O–Sn. This particular structure of deprotonated glucose molecule, attached to Sn defect site was taken as the starting structure to simulate the C_2–C_1 hydride transfer step (*cf* Fig. 1b). The size of the simulation cell was 18×14.5×16 Å^3. After the reactant and catalyst system was placed in the simulation cell, remaining space was completely filled with either water or methanol molecules.

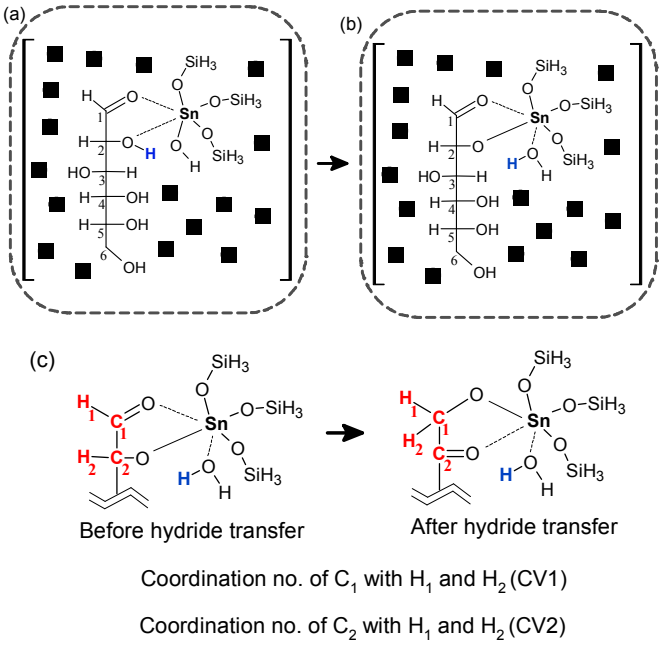

Figure 1: (a) Glucose coordinated with Sn–beta cluster model, representing the active catalyst site, via C_1 carbonyl and C_2 hydroxyl groups. Sn is octahedrally coordinated with 6 oxygen atoms. (b) Deprotonated glucose attached to Sn via C_2 oxygen. The proton from the C_2 hydroxyl group of glucose is taken by the –OH group attached to Sn to form a water molecule. This is the representation of the simulation cell. Black spheres represent solvent molecules in the simulation cell. (c) C_2 – C_1 Hydride transfer and the definition of collective variables CV1 and CV2, implemented in metadynamics. Atoms that form the collective variables are shown in red.

Ab initio molecular dynamics

Ab initio molecular dynamics (MD) simulations were performed using the CPMD package, version 3.15.1.[34] The CPMD package implements the Car–Parrinello scheme[35] for *ab initio* MD. The first–principles calculations were performed

using the planewave–pseudopotential implementation of Kohn–Sham density functional theory.[36] The Goedecker pseudopotential[33, 37] with local density approximation[36] was used. Only the *Γ*-point was used for integration over the Brillouin zone in the reciprocal space. An energy cut-off of 150 Ryd (2040.85 eV) proved sufficient to achieve energy convergence. Nosé-Hoover chain thermostat was used for controlling ionic and electronic temperatures. The frequency for the ionic thermostat was set to 1800 cm^{-1} (characteristic of a C–C bond vibration frequency) and for the electron thermostat to 10000 cm^{-1}. The fictitious electron mass parameter in CPMD was set to 1000 a.u. Short MD runs were performed without the thermostat to obtain an approximate value around which the electronic kinetic energy oscillates, and based on this observation, a value was chosen for subsequent simulations. The MD time step used in the simulation was 0.0964 fs. Geometry optimization was performed on the system before the MD run. Energies, including the fictitious electronic kinetic energy, were monitored to ascertain that the system did not deviate from the Born–Oppenheimer surface during the MD simulation. MD trajectories were visualized using the VMD software.[38]

CPMD simulations are computationally expensive and hence it is not feasible to run a simulation for experimental reaction timescales. The metadynamics technique[39-41] was thus implemented in conjunction with CPMD to accelerate the dynamics. It allows the construction of multidimensional free energy surfaces along selected reaction coordinates. This technique, as described by Laio and Gervasio,[40] is based on "filling up" the free energy surface by dropping potentials at small time intervals in the coordinate space of interest. The flattening of the free energy surface thus helps the system overcome activation energy barriers. The details of how metadynamics is implemented by extending the Car–Parrinello Lagrangian in CPMD can be found in the literature.[39] The implemented metadynamics collective variables (CV) to simulate the hydride transfer are defined in Fig. 1c. One hydrogen is bonded to each C_1 and C_2 before the hydride transfer and hence, CV1 ≈ CV2 ≈ 0.9. However, after the hydride transfer, CV1 is ≈ 1.8 and CV2 is ≈ 0.1 (*cf* Fig. 1c). Parameters in metadynamics were not optimized for the system studied in this paper, but general guidelines provided in the literature[42, 43] were followed. The height of the metadynamics potential was kept fixed at 1.25 kJ. Analogous to the original Car–Parrinello scheme, the dynamics of the collective variables were separated from the ionic and fictitious electronic motion by choosing an appropriate value for the fictitious mass of the collective variables. The temperature of the collective variables is set to 350 K (same as the physical temperature of the system) and was controlled in a window of ± 200 K using velocity rescaling.

Quantum mechanical calculations without finite temperature dynamics and without explicit solvent molecules

Quantum mechanical calculations were performed using density functional theory (DFT), with the B3LYP functional. All the calculations were performed using Gaussian-09 suite.[44] The Lewis acid Sn center was treated using LANL2DZ effective core potential basis and 6-311++g(d) basis set was used for C, H, O and Si atoms. The theory (DFT with B3LYP) and basis sets implemented in our calculations have already been benchmarked against higher level quantum mechanical methods like MP2 and G4 and have shown to be sufficiently accurate to describe the energetics of the reaction.[1, 45-48] To account for the effect of solvent environment, calculations were performed in water dielectric and methanol dielectric media (SCRF; solvent=methanol/water, CPCM solvation model). Full geometry optimizations were performed for all the investigated structures. The hydride transfer transition state was confirmed to be a first-order saddle point by frequency calculations and an Intrinsic Reaction Coordinate calculation was also performed at the transition state. The simulation system was identical to that shown in Fig. 1b, except the presence of explicit solvent molecules.

Results and Discussion

Energetics of hydride transfer

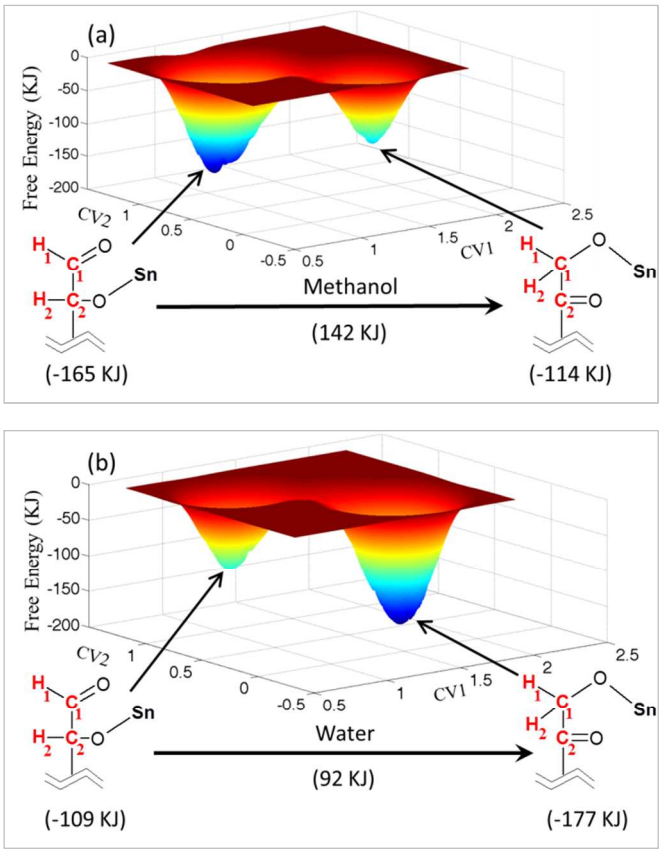

Figure 2: Metadynamics calculated free energy landscape for the hydride transfer from C_2 to C_1 in the presence of explicit, quantum mechanically treated (a) methanol and (b) water molecules. Structures corresponding to two minima in the free energy surface are shown. Only the metal center of the catalyst is shown for clarity purpose. The free energy barrier in the reaction step is shown below the arrow and free energies of the system before and after the hydride transfer are shown in parentheses. Refer to Fig. 1c for the definition of collective variables CV1 and CV2.

The CPMD–metadynamics computed free energy surfaces for the hydride transfer step, as a function of collective variables defined in Fig. 1c, in methanol and water, are shown in Fig. 2a and Fig. 2b, respectively. The free energy barrier for hydride transfer in methanol is 142 KJ/mol; whereas, it is 92 KJ/mol in water. It has to be noted that the apparent activation energy (enthalpy) barrier calculated experimentally for Sn–beta catalyzed isomerization in water, with hydride transfer as the

rate limiting step, is 93±15 KJ/mol.[15] However, no conversion of glucose to fructose in methanol was detected in the experiments. Additionally, it was also shown that SnO_2 particles, located externally on the zeolite, that catalyze the isomerization in methanol, do so via base catalyzed proton transfer, instead of hydride transfer.[15] These experimental results are in agreement with our computed free energy barriers, suggesting significantly higher activation energy barrier for the intramolecular hydride transfer in methanol than in water. Additionally, the free energy change associated with the hydride transfer in water ($\Delta G_{water} = -68$ KJ/mol) is significantly lower than in methanol ($\Delta G_{methanol} = +51$ KJ/mol).

Based on the knowledge in the existing literature, the reduction in the free energy barrier and in ΔG, in the case of water, could have been attributed to the following factors:

(i) *Water as a catalyst*: Li et al.[22] have shown that water molecule, if hydrogen bonded to the C_1 oxygen, can have synergistic effect of stabilizing the transition state (and possibly the product) since C_1 oxygen develops a higher negative charge during the hydride transfer step.[22, 45] However, a careful analysis of the CPMD–metadynamics trajectory did not reveal any water in the immediate vicinity of the C_1 oxygen that could provide this effect in the present work. To further confirm this, the hydride transfer step was also simulated, with CPMD–metadynamics, in the absence of any solvent, in vacuum. For this calculation, the size of the simulation cell was adjusted to keep more than 3 Å space between the outermost atom and the border of the simulation cell to avoid any artefacts. The free energy surface for hydride transfer in vacuum is shown in Fig. 3. As can be seen, the free energy barrier for hydride transfer in vacuum is slightly lower than that in water, i.e. 82 KJ/mol. The free energy change, ΔG_{vac}, is only −10.6 KJ/mol. Hence, in the present work, the possibility of water having a catalytic effect, via hydrogen bonding with the C_1 oxygen, can be ruled out.

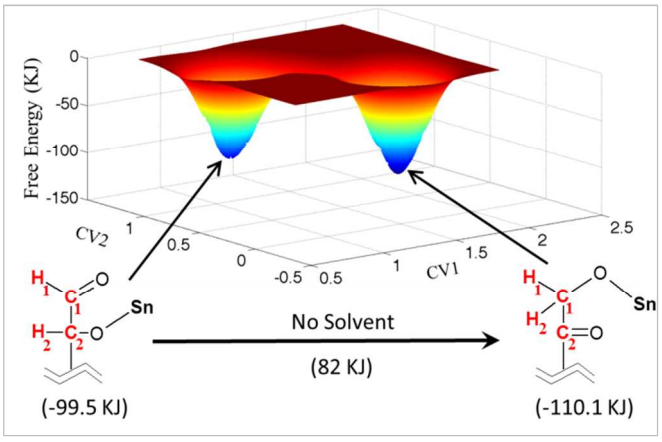

Figure 3: Metadynamics calculated free energy landscape for the hydride transfer from C_2 to C_1 in the absence of any solvent environment. Structures corresponding to two minima in the free energy surface are shown. Only the metal center of the catalyst is shown for clarity purpose. The free energy barrier in the reaction step is shown below the arrow and free energies of the system before and after the hydride transfer are shown in parentheses. Refer to Fig. 1c for the definition of collective variables CV1 and CV2.

(ii) *Implicit Solvent environment*: Water and methanol are polar solvents and water is more polar than methanol. This possibly gives rise to different implicit solvation environments for the reacting system in water and methanol. Hence, we simulated the hydride transfer step using DFT, in Gaussian–09, without finite temperature dynamics and using an implicit solvation model. The activation free energy barriers for hydride transfer in implicit water and methanol at 350 K (same temperature as that of CPMD–metadynamics calculations) are shown in Fig. 4. The free energy barrier computed in water (78.1 KJ/mol) is in good agreement with the previous computational literature.[1, 45] However, the free energy barrier and ΔG in methanol are almost the same as in water. In both the cases, the hydride transfer step is slightly exergonic. The comparison of the energetics of hydride transfer in implicit solvent (*cf* Fig. 4) and in explicitly treated solvent molecules, with finite temperature dynamics (*cf* Fig. 2), clearly suggest the role of solvent dynamics/reorientation/reorganization and/or solvent polarization and/or non–equilibrium solvation in the reaction.

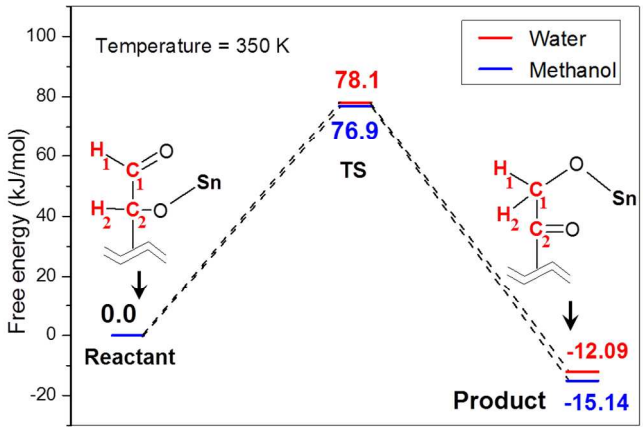

Figure 4: DFT calculated free energy barriers for hydride transfer from C_2 to C_1 in implicit solvation model and without finite temperature dynamics, as calculated using Gaussian-09.[44] Structures corresponding to the reactant and product are shown. Only the metal center of the catalyst is shown for clarity purpose. Product and transition state (TS) free energies are relative to that of the reactant.

Non–equilibrium solvation and solvent dynamics

Since methanol (polarizability = 3.29 Å^3) is more polarizable than water (polarizability = 1.45 Å^3)[49] and it's relaxation dynamics are slower than that of water,[50, 51] we provide the following explanation for the observed higher free energy barrier and endergonicity for hydride transfer in methanol, when solvent molecules are treated explicitly with finite temperature dynamics:

Out of multiple possible pathways,[52] the Sn–beta catalyzed intramolecular hydride transfer is suggested to be a concerted transfer of a neutral hydrogen from C_2 to C_1 and an electron transfer from C_2 oxygen to C_1 oxygen.[45] The charge transfer (and charge redistribution) within glucose would result in changing the electronic and orientational dipoles of the reacting system and this would polarize the solvent molecules.

However, since, methanol is more polarizable than water, the electron cloud of methanol gets more deformed than that of water, resulting in non–equilibrium solvation. The more pronounced electronic reorganization and non–equilibrium solvation of the transition state give rise to a higher free energy barrier for the reaction in methanol. Though the electronic polarization of methanol changes almost instantly during the hydride transfer, the nuclear orientational polarization/reorganization is a much slower process. Methanol molecules need to undergo higher degree of molecular reorientation than that of water molecules since their electronic cloud is more polarized. Hence, the free energy of the product state (after hydride transfer) in methanol is higher than that of the reactant state, as methanol needs to undergo significant orientational reorganization and that too over a larger timescale. Water, on the other hand, undergoes lesser electronic polarization and organizes itself relatively quickly to provide near equilibrium solvation to the transition state and an enhanced equilibrium solvation to the product state, after the hydride transfer.

We present the following results to support and validate this explanation:

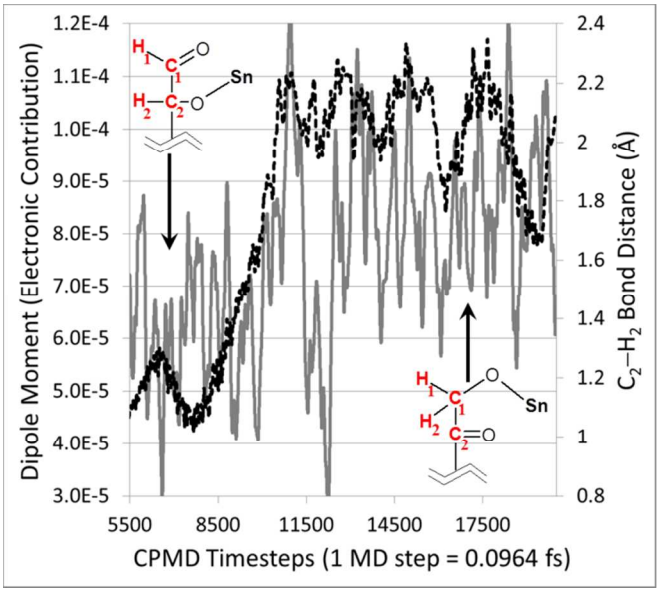

Figure 5: Variation of the electronic contribution of the dipole moment of the reactant and catalyst system during the hydride transfer step, as calculated during the CPMD–metadynamics simulation. The C_2–H_2 bond distance trajectory is also shown as a dotted line.

(i) The free energy barrier in vacuum, as shown in Fig. 3, is 60 KJ/mol lower than that in methanol and 10 KJ/mol lower than that in water. Since, there are no solvent molecules present in this simulation, the question of polarization/electronic reorganization of the solvent and of non–equilibrium solvation does not arise and hence the free energy barrier for the hydride transfer step is the lowest. Additionally, the free energies of the reactant and of the product states are not very different, since no reorientation or solvation effect is present either. The small difference in the free energy barriers in vacuum and in water also suggests that water molecules are getting polarized to a very small extent. This also implies that water molecules may have to reorient themselves only slightly after the hydride transfer.

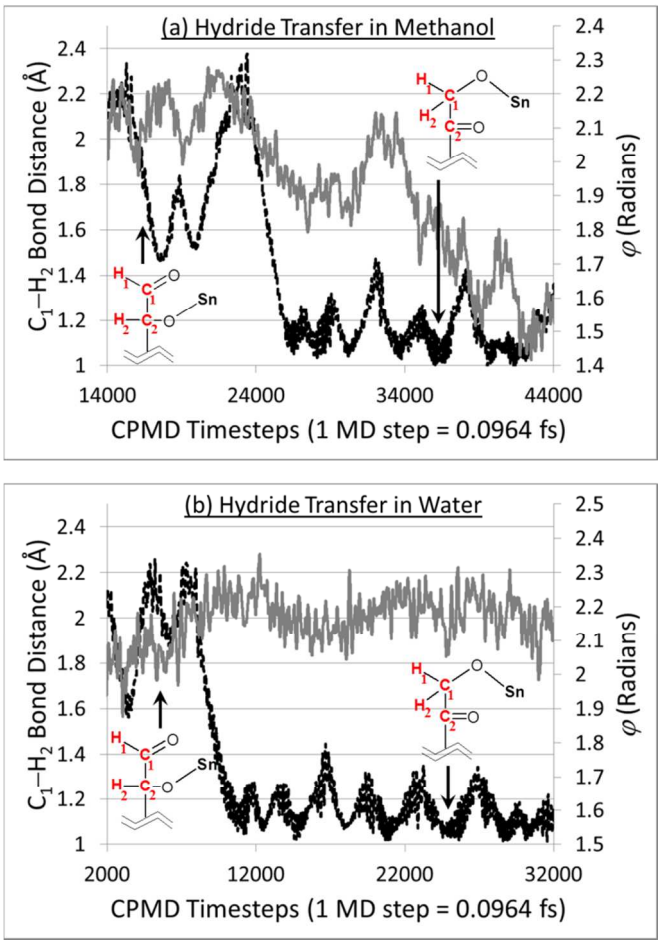

Figure 6: Variation in the orientation of the solvent dipole vector with respect to *z*–axis (or the angle that the solvent dipole vector makes with the *z*–axis of the simulation cell) during the hydride transfer step in the CPMD–metadynamics trajectory. (a) Methanol as the solvent, and (b) Water as the solvent. The C_1–H_2 bond distance along the trajectory is also shown as a dotted line.

(ii) Figure 5 shows the time evolution of the C_2–H_2 bond (dotted line) as the system (reactant glucose and the catalyst) undergoes hydride transfer. At the CPMD timestep of around 10,000, the C_2–H_2 separation increases from about 1.2 Å to about 2.1 Å, indicating the hydride transfer. The grey line in Fig. 5 shows the electronic contribution to the dipole moment of the reacting system in the course of this transition; as calculated using optimally localized Wannier functions,[53-55] as implemented in the CPMD code. Owing to the high computational cost that such a calculation entails, only the part of the trajectory from shortly before to shortly after the observed hydride transfer is shown. It can be seen in Fig. 5 that the hydride transfer is accompanied by a simultaneous change in the electronic polarization of the reactant and the catalyst system, and that this change in the polarization of the reacting system will change the electronic polarization of a solvent (to

different extents though) instantly, so as to keep it aligned with that of the reactant and the catalyst.

(iii) To analyze the (nuclear/molecular) orientational reorganization of solvent molecules during and after the hydride transfer step, we computed the orientational dipole of water and methanol molecules in the simulation system (by assigning partial charges to atoms in water and methanol molecules in the CPMD computed trajectory), along the CPMD–metadynamics trajectory. Figures 6a and 6b show the time evolution of the C_1–H_2 bond (dotted line) as the system undergoes hydride transfer in methanol and water, respectively. The dynamics of the orientation of the solvent dipole vector with respect to *z*–axis (angle that the dipole vector makes with the *z*–axis of the simulation cell) along the trajectory are also shown (grey line) for both the solvents. It can be seen in Fig. 6b that the orientation of the dipole vector for water changes only slightly when the hydride transfer is initiated, but does not change even 20,000 MD steps (2 ps) after the hydride transfer. However, as can be seen in Fig. 6a, a systematic and gradual change in the orientation of the dipole vector of methanol, over the period of 2 ps after the hydride transfer, is observed. This clearly shows that methanol molecules undergo a significant reorientation after the hydride transfer; whereas, there is hardly any change in the average orientation of water molecules after the hydride transfer. Additionally, oscillations in the dipole vector's orientation in water are more systematic, with a higher frequency and lower magnitude. This suggests that whatever little reorientation water has to go through will be done at a shorter timescale. This will enable nearer to equilibrium solvation environment to the transition state and an equilibrium solvation environment after the hydride transfer. The change in the orientation of the solvent dipole vector with respect to *x* and *y* axes is also provided as supporting information (refer to Figs. S2 and S3). No change in the orientation of water is observed (Figs. S2b and S3b). For methanol, a slight change along the *x* axis is seen.

(iv) An additional simulation of the hydride transfer in methanol was performed, with lesser time given to the solvent molecules to relax. This was achieved by allowing only 50 CPMD steps to be performed in between metadynamics steps in these simulations. As can be seen in the corresponding free energy surface in Fig. 7, the barrier for hydride transfer increases only by 10 KJ/mol; whereas the change in the free energy, ΔG, increases from 51 KJ/mol (*cf* Fig. 2a) to 140 KJ/mol (*cf* Fig. 7). As suggested earlier, since the barrier for hydride transfer is a result of the electronic reorganization of the solvent and the non–equilibrium solvation of the transition state, it does not change significantly in this case, since the electronic polarization of the solvent is an instantaneous process. However, since, the (nuclear) reorientation of methanol is a much slower process, and we do not allow sufficient time for the methanol molecules to relax/reorient (to adjust themselves to the changed electronic environment) in this case, the free energy of the product state is significantly higher, making it relatively unstable. Similar simulation was also performed for hydride transfer in water and the effect of not allowing water molecules to relax on the free energy of the product state was significantly less pronounced (refer to Fig. S1 in the supporting information) since, the electronic polarization in water is lesser than that of methanol and lesser molecular reorientation of water is required.

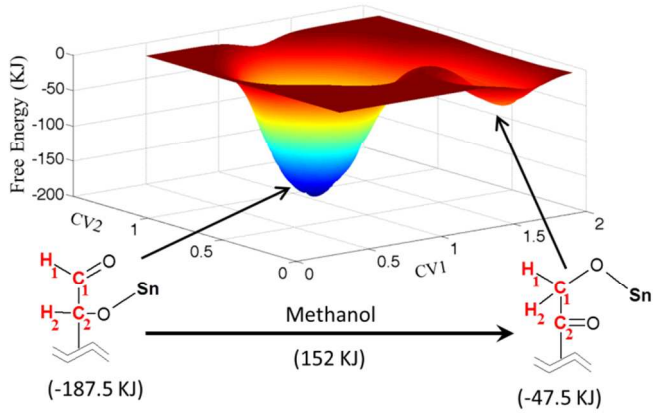

Figure 7: Metadynamics calculated free energy landscape for the hydride transfer from C_2 to C_1 in the presence of explicit, quantum mechanically treated methanol molecules. Structures corresponding to two minima in the free energy surface are shown. Only the metal centre of the catalyst is shown for clarity purpose. The free energy barrier in the reaction step is shown below the arrow and free energies of the system before and after the hydride transfer are shown in parentheses. Refer to Fig. 1c for the definition of collective variables CV1 and CV2. It has to be noted that, unlike Fig. 2a, methanol molecules in this case get significantly lesser time to relax along the CPMD–metadynamics trajectory.

Analogy to enzyme catalyzed charge transfer reactions

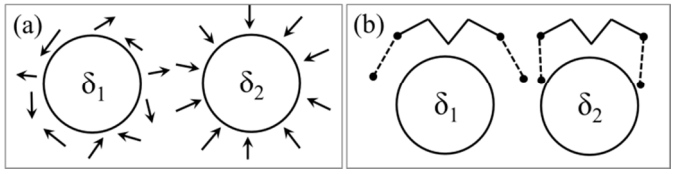

Figure 8: Illustration of the (a) orientation of solvent dipoles and (b) the (pre)organization of the charged groups of enzymes. δ_1 and δ_2 indicate two different charge configurations. As the charge configuration changes from δ_1 to δ_2, solvent dipoles have to reorganize significantly; whereas the preorganized charge groups of the enzyme have to undergo minimal change in the orientation to adjust itself to the change. Adapted from Warshel and co-workers.[56, 57]

In addition to the explanation provided above, the energetics of intra–molecular hydride transfer in water and methanol can also be discussed in a fashion analogous to that of enzyme catalyzed charge transfer reactions, as explained by Warshel and co–workers.[56-60] They showed that enzymes can stabilize different charged groups by fixing their dipoles in appropriate orientations and hence they do not have to undergo significant structural reorientation as the charge transfer happens. The active site dipoles are preorganized towards the changed charge structure. Here preorganization refers to the alignment of the polar charged groups of the enzyme via electrostatic interactions with the reacting structure, prior to the charge transfer. Because of this preorganization, they have to undergo minimal reorientation, as the charge distribution on the reacting structure gets altered (*cf* Fig. 8b for illustration). In many cases,

the reduction in the activation free energy is achieved mainly because of the preorganization of the active site permanent dipoles of the enzyme that allows the enzyme to stabilize the transition and the product state significantly better than that of any solvent. Contrary to the enzyme, solvent dipoles are less systematically oriented. The enzymes may not always reduce the Marcus reorganization energy (see Fig. 9 for a graphical explanation of Marcus reorganization energy, denoted as λ) to bring down the free energy activation barrier, but it is an effect of lowering the free energy change (ΔG) of the reaction. Solvents on the other hand, have to undergo significant molecular reorientation during the charge transfer process and hence cannot stabilize the product (and the transition state) as well as enzymes do. Refer to Fig. 8 for an illustration.

In the intramolecular hydride transfer step studied in this paper, we observe that methanol has to undergo significant molecular reorientation over a larger timescale since it undergoes more electronic polarization; whereas, little or no significant polarization, resulting in very little and relatively faster reorientation in water allows it to solvate the reactant, during and after the hydride transfer, better. The stability effect which is provided by enzymes due to electrostatic interactions is provided by water, in this case, by the virtue of its lower polarizability and relatively faster dynamics.

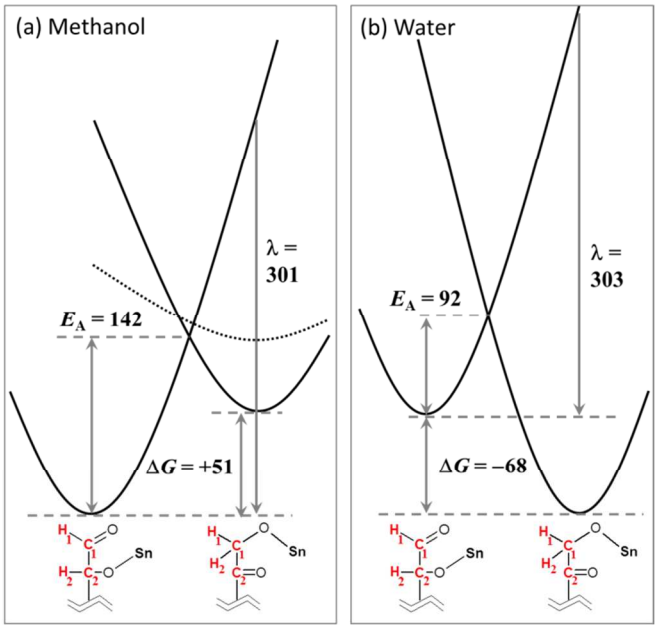

Figure 9: An illustration of the reduction in the activation free energy barrier of the hydride transfer step in water due to the reduction in the free energy change associated with the step. The fact that, unlike methanol, water molecules do not have to reorient themselves after the hydride transfer leads to lower ΔG for the reaction in water. Marcus reorganization energy does not change significantly. The dotted black line represents the free energy surface for the simulation in which methanol molecules were not allowed to relax completely. All free energy values are in KJ/mol.

To further confirm this, the minimum free energy pathways for hydride transfer in methanol and water, in the free energy surfaces shown in Figs. 2a and 2b, respectively, were traced to get 2–dimensional free energy profiles. Extrapolating the reactant (before hydride transfer) and product (after hydride transfer) free energy wells, the Marcus reorganization energy, λ, was calculated for both, methanol and water. As illustrated in Fig. 9, the reorganization energy is almost the same for water and methanol. The reduction in the activation energy barrier in water is due to improved solvation (equilibrium solvation, little or no polarization) of the product state and of the transition state by water than by methanol (non–equilibrium solvation, significant reorientation required). Similar to that of enzymes, water "(pre)organizes" itself to better solvate the product.

Conclusions

The effect of solvent environment on the intramolecular hydride transfer reaction in biomass molecules was studied using glucose to fructose isomerization as an example. The C_2–C_1 hydride transfer step, catalyzed by Sn–beta, was simulated in the presence of explicit solvent molecules, with finite temperature dynamics, using Car–Parrinello molecular dynamics (CPMD) and metadynamics. Hydride transfer was also simulated in an implicit solvent environment using density functional theory (DFT). Unlike DFT calculations in implicit solvent, where the free energy activation barrier was the same for water and methanol, the free energy activation barrier calculated by CPMD–metadynamics was found to be 50 KJ/mol higher in methanol than in water. The free energy barrier in vacuum was found to be slightly lower than that in water. Analysis of the electronic polarization of the reactant and the catalyst system and that of the reorientation of solvent molecules along the CPMD–metadynamics trajectories suggest that due to higher polarizability of methanol than water, the change in the charge structure of the reactant polarizes methanol to a greater extent. The electronic polarization of methanol results in non–equilibrium solvation of the transition state. This gives rise to higher activation free energy barrier in methanol. Additionally, the electronic polarization in methanol necessitates significant reorientation of methanol molecules after the hydride transfer step and methanol has relatively slower relaxation dynamics. Thus, the product state (after hydride transfer) is solvated poorly. On the contrary, water would not undergo significant polarization and hence requires very little reorientation during the hydride transfer. Thus, water provides enhanced, (near) equilibrium solvation for the transition state and to the product state. The aforementioned explanation was also juxtaposed with the mechanism of charge transfer reactions catalyzed by enzymes. Enzymes can lower the free energy activation barrier of charge transfer reactions by preorganizing around the charged moieties by providing electrostatic stabilization to the products. They reduce the free energy change of the reaction, without altering the reorganization energy λ to a great extent. Similarly, in this case, water lowers the activation free energy of the hydride transfer reaction by not getting polarized as much as methanol and providing better solvation environment to the product and to the transition state, thereby significantly reducing the free energy change of the hydride transfer step.

Acknowledgements

Financial support by the Singapore Ministry of Education Academic Research Fund (MOE–AcRF) Tier–1 grant (RGT36/13) is acknowledged. JJV acknowledges the research scholarship by Nanyang Technological University, Singapore. SHM would like to thank Dr. Stavros Caratzoulas for many insightful discussions (related to solvent dynamics) that happened during his post–doctoral tenure in the Catalysis Centre for Energy Innovation (CCEI) at the University of Delaware.

Notes and references

[a] School of Chemical and Biomedical Engineering, Nanyang Technological University, 62 Nanyang Drive, Singapore 637459.

* Corresponding author email: SHMushrif@ntu.edu.sg (SHM)

† JJV provided help in running CPMD–metadynamics simulations on NTU High Performance Computing Cluster, in reconstructing the free energy surfaces and in editing the paper. CBK performed quantum mechanical DFT calculations in Gaussian–09 suite to simulate hydride transfer in an implicit solvent environment.

Electronic Supplementary Information (ESI) available: (i) Metadynamics calculated free energy surface for hydride transfer simulated in explicit water, but with lesser time for the solvent molecules to relax. (ii) Variation in the orientation of the solvent (water and methanol) dipole vector (with respect to *x* and *y* axes) during the hydride transfer step in the CPMD–metadynamics trajectory. See DOI: 10.1039/b000000x/

1. R. Bermejo-Deval, R. S. Assary, E. Nikolla, M. Moliner, Y. Román-Leshkov, S. J. Hwang, A. Palsdottir, D. Silverman, R. F. Lobo, L. A. Curtiss and M. E. Davis, *Proceedings of the National Academy of Sciences of the United States of America*, 2012, **109**, 9727-9732.
2. M. Moliner, Y. Roman-Leshkov and M. E. Davis, *Proceedings of the National Academy of Sciences of the United States of America*, 2010, **107**, 6164-6168.
3. Y. Roman-Leshkov, M. Moliner, J. A. Labinger and M. E. Davis, *Angew Chem Int Edit*, 2010, **49**, 8954-8957.
4. S. Caratzoulas and D. G. Vlachos, *Carbohyd Res*, 2011, **346**, 664-672.
5. N. Nikbin, S. Caratzoulas and D. G. Vlachos, *Chemcatchem*, 2012, **4**, 504-511.
6. X. Qian and X. Wei, *The journal of physical chemistry. B*, 2012, **116**, 10898-10904.
7. S. H. Mushrif, J. J. Varghese and D. G. Vlachos, *Physical Chemistry Chemical Physics*, 2014, **16**, 19564-19572.
8. V. Choudhary, A. B. Pinar, R. F. Lobo, D. G. Vlachos and S. I. Sandler, *Chemsuschem*, 2013, **6**, 2369-2376.
9. N. Guo, S. Caratzoulas, D. J. Doren, S. I. Sandler and D. G. Vlachos, *Energy & Environmental Science*, 2012, **5**, 6703-6716.
10. Y. Román-Leshkov, J. N. Chheda and J. A. Dumesic, *Science*, 2006, **312**, 1933-1937.
11. P. Azadi, R. Carrasquillo-Flores, Y. J. Pagán-Torres, E. I. Gürbüz, R. Farnood and J. A. Dumesic, *Green Chemistry*, 2012, **14**, 1573.
12. J. M. R. Gallo, D. M. Alonso, M. A. Mellmer and J. A. Dumesic, *Green Chemistry*, 2013, **15**, 85.
13. J. M. R. Gallo, D. M. Alonso, M. A. Mellmer, J. H. Yeap, H. C. Wong and J. A. Dumesic, *Topics in Catalysis*, 2013, **56**, 1775-1781.
14. E. I. Gurbuz, S. G. Wettstein and J. A. Dumesic, *Chemsuschem*, 2012, **5**, 383-387.
15. R. Bermejo-Deval, R. Gounder and M. E. Davis, *Acs Catalysis*, 2012, **2**, 2705-2713.
16. S. H. Mushrif, S. Caratzoulas and D. G. Vlachos, *Physical Chemistry Chemical Physics*, 2012, **14**, 2637-2644.
17. S. K. R. Patil and C. R. F. Lund, *Energy & Fuels*, 2011, **25**, 4745-4755.
18. G. Tsilomelekis, T. R. Josephson, V. Nikolakis and S. Caratzoulas, *Chemsuschem*, 2014, **7**, 117-126.
19. V. Nikolakis, S. H. Mushrif, B. Herbert, K. S. Booksh and D. G. Vlachos, *The journal of physical chemistry. B*, 2012, **116**, 11274-11283.
20. S. Caratzoulas, T. Courtney and D. G. Vlachos, *J Phys Chem A*, 2011, **115**, 8816-8821.
21. B. N. Zope, D. D. Hibbitts, M. Neurock and R. J. Davis, *Science*, 2010, **330**, 74-78.
22. G. Li, E. A. Pidko and E. J. M. Hensen, *Catalysis Science & Technology*, 2014, **4**, 2241-2250.
23. X. Qian and D. Liu, *Carbohydr Res*, 2014, **388**, 50-60.
24. M. A. Mellmer, C. Sener, J. M. R. Gallo, J. S. Luterbacher, D. M. Alonso and J. A. Dumesic, *Angewandte Chemie International Edition*, 2014, **53**, 11872-11875.
25. S. Feng, C. Bagia and G. Mpourmpakis, *The Journal of Physical Chemistry A*, 2013, **117**, 5211-5219.
26. S. H. Mushrif, V. Vasudevan, C. B. Krishnamurthy and B. Venkatesh, *Chemical Engineering Science*, 2015, **121**, 217-235.
27. K. L. Fleming and J. Pfaendtner, *The Journal of Physical Chemistry A*, 2013, **117**, 14200-14208.
28. A. I. Torres, P. Daoutidis and M. Tsapatsis, *Energy & Environmental Science*, 2010, **3**, 1560-1572.
29. S. H. Bhosale, M. B. Rao and V. V. Deshpande, *Microbiological reviews*, 1996, **60**, 280-300.
30. A. Corma, M. E. Domine, L. Nemeth and S. Valencia, *Journal of the American Chemical Society*, 2002, **124**, 3194-3195.
31. M. J. Climent, A. Corma and S. Iborra, *Green Chemistry*, 2011, **13**, 520-540.
32. J. N. Chheda, Y. Roman-Leshkov and J. A. Dumesic, *Green Chemistry*, 2007, **9**, 342-350.
33. C. Hartwigsen, S. Goedecker and J. Hutter, *Phys Rev B*, 1998, **58**, 3641-3662.
34. X. Qian, M. R. Nimlos, M. Davis, D. K. Johnson and M. E. Himmel, *Carbohydr Res*, 2005, **340**, 2319-2327.
35. R. Car and M. Parrinello, *Physical review letters*, 1985, **55**, 2471-2474.
36. W. Kohn and L. J. Sham, *Physical Review*, 1965, **140**, 1133-&.
37. S. Goedecker, M. Teter and J. Hutter, *Physical review. B, Condensed matter*, 1996, **54**, 1703-1710.
38. W. Humphrey, A. Dalke and K. Schulten, *J Mol Graph Model*, 1996, **14**, 33-38.
39. M. Iannuzzi, A. Laio and M. Parrinello, *Physical review letters*, 2003, **90**.

40. A. Laio and F. L. Gervasio, *Rep Prog Phys*, 2008, **71**.
41. A. Laio and M. Parrinello, *Proceedings of the National Academy of Sciences of the United States of America*, 2002, **99**, 12562-12566.
42. B. Ensing, A. Laio, M. Parrinello and M. L. Klein, *The journal of physical chemistry. B*, 2005, **109**, 6676-6687.
43. A. Laio, A. Rodriguez-Fortea, F. L. Gervasio, M. Ceccarelli and M. Parrinello, *The journal of physical chemistry. B*, 2005, **109**, 6714-6721.
44. M. J. T. Frisch, G. W.; Schlegel, H. B.; Scuseria, G. E.; Robb, M. A.; Cheeseman, J. R.; Scalmani, G.; Barone, V.; Mennucci, B.; Petersson, G. A.; Nakatsuji, H.; Caricato, M.; Li, X.; Hratchian, H. P.; Izmaylov, A. F.; Bloino, J.; Zheng, G.; Sonnenberg, J. L.; Hada, M.; Ehara, M.; Toyota, K.; Fukuda, R.; Hasegawa, J.; Ishida, M.; Nakajima, T.; Honda, Y.; Kitao, O.; Nakai, H.; Vreven, T.; Montgomery, Jr., J. A.; Peralta, J. E.; Ogliaro, F.; Bearpark, M.; Heyd, J. J.; Brothers, E.; Kudin, K. N.; Staroverov, V. N.; Kobayashi, R.; Normand, J.; Raghavachari, K.; Rendell, A.; Burant, J. C.; Iyengar, S. S.; Tomasi, J.; Cossi, M.; Rega, N.; Millam, N. J.; Klene, M.; Knox, J. E.; Cross, J. B.; Bakken, V.; Adamo, C.; Jaramillo, J.; Gomperts, R.; Stratmann, R. E.; Yazyev, O.; Austin, A. J.; Cammi, R.; Pomelli, C.; Ochterski, J. W.; Martin, R. L.; Morokuma, K.; Zakrzewski, V. G.; Voth, G. A.; Salvador, P.; Dannenberg, J. J.; Dapprich, S.; Daniels, A. D.; Farkas, Ö.; Foresman, J. B.; Ortiz, J. V.; Cioslowski, J.; Fox, D. J. , Gaussian, Inc., Wallingford CT, Editon edn., 2009.
45. V. Choudhary, S. Caratzoulas and D. G. Vlachos, *Carbohyd Res*, 2013, **368**, 89-95.
46. N. Rai, S. Caratzoulas and D. G. Vlachos, *Acs Catalysis*, 2013, **3**, 2294-2298.
47. M. Boronat, A. Corma, M. Renz, G. Sastre and P. M. Viruela, *Chem-Eur J*, 2005, **11**, 6905-6915.
48. R. S. Assary and L. A. Curtiss, *J Phys Chem A*, 2011, **115**, 8754-8760.
49. D. R. Lide, ed., *CRC Handbook of Chemistry and Physics, Internet Version 2005*, CRC Press, Boca Raton, FL, 2005.
50. K. Ando and S. Kato, *The Journal of Chemical Physics*, 1991, **95**, 5966-5982.
51. T. Ishida, F. Hirata and S. Kato, *The Journal of Chemical Physics*, 1999, **110**, 11423-11432.
52. S. Hammes-Schiffer, *ChemPhysChem*, 2002, **3**, 33-42.
53. N. Marzari and D. Vanderbilt, *Phys Rev B*, 1997, **56**, 12847-12865.
54. P. L. Silvestrelli, *Phys Rev B*, 1999, **59**, 9703-9706.
55. G. Berghold, C. J. Mundy, A. H. Romero, J. Hutter and M. Parrinello, *Phys Rev B*, 2000, **61**, 10040-10048.
56. A. Warshel, *Proceedings of the National Academy of Sciences*, 1978, **75**, 5250-5254.
57. A. Warshel, P. K. Sharma, M. Kato, Y. Xiang, H. Liu and M. H. M. Olsson, *Chemical Reviews*, 2006, **106**, 3210-3235.
58. A. Yadav, R. M. Jackson, J. J. Holbrook and A. Warshel, *Journal of the American Chemical Society*, 1991, **113**, 4800-4805.
59. J. Villà and A. Warshel, *The Journal of Physical Chemistry B*, 2001, **105**, 7887-7907.
60. A. Warshel and W. W. Parson, *Quarterly Reviews of Biophysics*, 2001, **34**, 563-679.